

40 Referring to Hughes (2008), Van der Veen (2016) states on his page 1332 that I believe
41 lateral drag vanishes at the center of an ice stream. Lateral shear stress σ_{xy} vanishes, but
42 the lateral shear force does not. On one side, stress σ_{xy} acts on side area A_y and on the
43 other side stress $-\sigma_{xy}$ acts on side area $-A_y$, with A_y and $-A_y$ being vectors in opposite y
44 directions, so the shear force is always positive and opposes longitudinal gravitational
45 forcing.

46 Van der Veen (2016) states his Eq. (9) is my Eq. (36) in Hughes (2003). It is not, his
47 signs are different from mine and his σ_F is not the same as my σ_f . In the geometric force
48 balance, the driving force is the area of a triangle and all the resisting forces are areas of
49 triangles and a rectangle (or parallelogram) that fit into the triangle so the driving and
50 resisting forces are identical. All signs are positive in my Eq. (36). His σ_F is my flotation
51 stress, which doesn't appear in my 2003 paper. It appears in my Nova book, *Holistic Ice*
52 *Sheet Modeling* (Hughes, 2012a) and in Hughes et al. (2016) in *The Cryosphere*. Van der
53 Veen (page 1333) states my σ_F is his \tilde{R}_{xx} . It is not. His force budget approach has no way
54 for calculating my flotation stress σ_f because his approach has no place for my floating
55 fraction ϕ of ice under an ice stream (which he calls a "basal buoyancy factor" that
56 obscures its physical meaning), see my Fig. 1.

57 Van der Veen (2016) states his Eqs. (13), (14), and (15) are my equations in my 2008,
58 2012a, and 2016 publications. They are not. His signs are different from mine and even
59 some of his terms are different from mine. The proof is found by substituting his Eqs. (13)
60 through (15) into his Eq. (9), which does not deliver $0 = 0$ for the force balance. My
61 equations, reproduced as my Table 1 from Table 12.1 in Hughes (2012a), do give $0 = 0$. In
62 my geometric force balance, resisting forces are represented by triangles and a rectangle
63 (or parallelogram) that exactly fit inside a big right triangle that represents my driving
64 force, so the area of my big triangle is the same as summed component areas from resisting
65 forces within it. Therefore $0 = 0$ must be obtained, see my Fig. 2.

66 Van der Veen (2016) plots his Eqs. (9) through (15) in his Fig. 2, so they cannot
67 represent my force balance because they are not my equations. Also the plot of his
68 "Gradients in longitudinal stress" should be gradients in longitudinal force, which is a
69 stress, so he can compare stresses with stresses, not with stress gradients of stresses. If his
70 Fig. 2 truly plots a longitudinal stress gradient, it compares apples with oranges. Also in his
71 Fig. 2, his longitudinal stress (or force) gradient acts in the same direction as his
72 gravitational driving force. That is impossible in my geometric force balance, see my Fig. 2.

73 Referring to my Figure 3 (left), Figure 3 in Van der Veen (2016), line AF should be
74 parallel to line BE because they both show ice pressure increasing linearly with depth. Line
75 CE shows how water pressure increases linearly with depth, as is obvious at the calving
76 front. In my geometrical force balance, the longitudinal gravitational driving force is area
77 ADF of the big triangle. Fitted inside ADF are a resisting flotation force given by area BDE
78 for floating ice fraction ϕ and a resisting drag force given by area ABEF for the grounded
79 ice fraction $1 - \phi$ in my Fig. 1. Inside BDE is area CDE for the resisting force from water

80 pressure and area BCE for the resisting force from the tensile strength of ice. Inside area
81 ABEF is the triangle above B for basal drag and the parallelogram below B for side drag.
82 Resistance from basal drag is the area of the triangle above B. Resistance from side drag is
83 the area of the parallelogram below B if lines BE and AF are made parallel. If BE is made
84 part of AF a rectangle would replace the parallelogram but the area would be unchanged,
85 see my Fig. 2. That's all there is to it. The only remaining task is to replace forces with
86 products of stresses and lengths (for areas having unit or constant widths along x) upon
87 which the stresses act along a flowline (no width) or a flowband (constant width). My
88 solution for the force balance is exact because forcing area ADF equals resisting areas
89 ABEF, BCE, and CDE inside ADF. All gravitational and resisting forces in the longitudinal
90 direction of ice flow are thereby included, with ABEF representing the force from both
91 basal and side drag.

92 Van der Veen (2016) correctly states his Eq. (16) represents my longitudinal
93 gravitational driving force, but then he states it "does not represent the gravitational
94 driving force" (page 1335). It does. In my direction $-x$ of ice flow, the gravitational force (a
95 horizontal vector) is the average ice pressure (a scalar) times the transverse cross-
96 sectional area against which it acts (as a horizontal vector in my $-x$ direction), which for
97 an ice stream of constant width is ice width times ice height above the bed, a height that
98 varies along x , as does average ice pressure, so the gravitational driving force varies along
99 x . The correct representation of my longitudinal geometric force balance is my Fig. 2 where
100 his area ABEF is my area 1+2 for basal and side drag at x .

101 Van der Veen (2016) states on his page 1335 that a longitudinal force balance along x
102 must be made over incremental distance Δx that shrinks to zero. My longitudinal force
103 balance along x does in my Fig. 2 (bottom), see Hughes (2012a, Appendix G) and Hughes et
104 al. (2016, page 10). I subtract longitudinal force areas over distance Δx to get my
105 longitudinal force balance Eq. (22) in Hughes et al. (2016). However, Van der Veen (2016)
106 is incorrect in stating a longitudinal force balance *always* must be made over length Δx . At
107 the calving front of an ice shelf the balance is obtained right at the calving front where
108 $\Delta x = 0$, as Robin (1958) proved 59 years ago *geometrically*.

109 Van der Veen (2016) discusses areas ADF and APD in terms of "lithostatic stresses"
110 increasing with depth in his Fig. 4(a), shown in my Fig. 3 (right). The areas are forces. As he
111 shows by his horizontal arrows in his Fig. 4(a), area ADF is my horizontal gravitational
112 driving force and area APD is the sum of my horizontal resisting forces opposing the
113 driving force in my geometrical force balance shown in my Fig. 2 (center) with an ice
114 surface slope at x . His area APD can be subdivided into my smaller areas of triangles and a
115 rectangle in my Fig. 2 (center) to obtain areas that resist gravitational forcing from his area
116 ADF. There is no surface slope in his Fig. 4(a), a condition that applies to an unconfined
117 linear ice shelf having constant thickness (Weertman, 1957; Robin, 1958), in which case
118 only my areas 3 and 4 in my Fig. 2 (bottom) add to give his area APD since there are no
119 basal and side drag forces represented by my areas 1 and 2. Raymond (1982) analyzed
120 deformation near interior ice divides where the surface slope is also zero.

121 Van der Veen (2016) correctly shows the geometrical force balance in my Fig. 2
122 (bottom) for a sloping ice surface above a horizontal bed in his Fig. 4(b), shown in my Fig. 3

123 (right). From these figures we can both obtain the geometric longitudinal force balance
 124 over incremental length Δx in analytic form when $\Delta x \rightarrow 0$. In my Fig. 2 (bottom), my big
 125 triangles at x and $x + \Delta x$ are gravitational driving forces that are respectively subdivided
 126 into areas 1, 2, 3, 4 and areas 5, 6, 7, 8 that resist gravitational motion along x .

127 **My Geometrical Force Balance**

128 I developed the geometrical force balance to teach the fundamentals of glaciology to
 129 students with an inadequate background in mathematics, usually students studying to be
 130 glacial geologists (Hughes, 2012a). My geometrical approach was designed to make
 131 maximum use of glacial geology in reconstructing former ice sheets from the bottom up
 132 (Hughes, 1998, Chapters 9 and 10; Fastook and Hughes, 2013) and in demonstrating how
 133 basal thermal conditions produce glacial geology under the Antarctic Ice Sheet today
 134 (Hughes, 1998, Chapter 3, Wilch and Hughes, 2000; Siegert, 2000). Previously I had spent
 135 more time teaching calculus than glaciology because the Navier-Stokes equations had to be
 136 integrated in the force balance.

137 The major variable in my geometrical force balance is the floating fraction ϕ of ice,
 138 where $\phi = 0$ for sheet flow, $0 < \phi < 1$ for stream flow, and $\phi = 1$ for shelf flow. Here we are
 139 primarily interested in stream flow as shown in my Fig. 1 for possible ϕ distributions at
 140 the bed and my Fig. 2 for the longitudinal force balance. From Newton's second law of
 141 motion in a vertical force balance, gravitational force F_G at the base must be the same for
 142 floating area $w_F \Delta x$ and total area $w_I \Delta x$ such that $F_G = (\rho_I h_I w_I \Delta x)g = (\rho_I h_F w_F \Delta x)g$ for ice
 143 density ρ_I and gravity acceleration g to obtain basal pressures $P_F = \rho_I g h_F$ and $P_I = \rho_I g h_I$
 144 that support ice of respective floating and total heights h_F and h_I . This vertical force
 145 balance is satisfied if h_F goes from 0 to h_I as w_F goes from 0 to w_I . The basal water
 146 pressure is $P_W = \rho_W g h_W = P_F = \rho_I g h_F$ for water density ρ_W and water height h_W needed to
 147 float ice height h_F . The floating fraction of ice at x is therefore:

$$148 \quad \phi = w_F / w_I = h_F / h_I = P_F / P_I = P_W / P_I.$$

149 Pulling force $\sigma_T h_I$ resists the gravitational driving force given by area 4 in Figure 2
 150 (bottom), which is area 3+4 minus area 3. Area 3+4 is one-half flotation height $h_F = h_I \phi$
 151 times basal floating length $P_F = P_I \phi$, so area 3+4 is $\bar{P}_I h_I \phi^2$. Area 3 is one-half height
 152 $h_W = (\rho_I / \rho_W) h_F = (\rho_I / \rho_W) h_I \phi$ times the same basal floating length $P_F = P_I \phi$. Then the
 153 tensile pulling stress is $\sigma_T = \bar{P}(1 - \rho_I / \rho_W) \phi^2$. It is that simple. At the calving front where
 154 $\phi = 1$ this is the solution obtained by Weertman (1957) and Robin (1958). Table 1 lists all
 155 stresses resisting gravitational forcing at x .

156 At distance x from the ice-shelf grounding line in my Fig. 2, gravitational driving force
 157 $F_G = \bar{P}_I h_I$ is resisted by the sum of upstream tensile pulling force $F_T = \sigma_T h_I$ and
 158 downstream compressive pushing force $F_C = \sigma_C h_I$ so $\sigma_T = \bar{P}_I - \sigma_C$. Tensile force $\sigma_T h_I$
 159 balances the part of the driving force equal to area 4, and resisting force $\sigma_C h_I$ balances the

160 part of the driving force equal to areas 1+2+3 in Figure 2 (center and bottom), and includes
 161 all downstream resistance due to averaged basal and side shear stresses $\bar{\tau}_o$ and $\bar{\tau}_s$
 162 respectively linked to areas 1 and 2, plus local water buttressing stress σ_w linked to area 3,
 163 all of which resist gravitational forcing equivalent to these areas.

164 My geometrical force balance is shown in Fig. 2, which is Fig. 5 in Hughes et al. (2016).
 165 Along incremental length Δx , change ΔF_G in the longitudinal gravitational driving force F_G
 166 is balanced by change ΔF_T in the tensile pulling force F_T plus change ΔF_W in the water
 167 buttressing force F_W plus basal drag force F_O plus side drag force F_S , where $F_F = F_T + F_W$
 168 is a flotation force that requires ice-bed uncoupling by basal water. Dividing by Δx and
 169 letting $\Delta x \rightarrow 0$ gives as the longitudinal gravitational force gradient

$$170 \quad \partial F_G / \partial x = \partial(\bar{P}_I h_I) / \partial x = P_I \alpha_I = \partial(\sigma_F h_I) / \partial x + \tau_o + 2\tau_s (h_I / w_I)$$

171 where the bed is represented by an up-down staircase with successive Δx steps so ice
 172 thickness gradient α_I equals α for ice surface slope on each step, P_I is the overburden ice
 173 pressure at the base, τ_o is the basal shear stress, τ_s is the side shear stress for two sides,
 174 h_I is ice thickness, h_w is the height of water that floats flotation height h_F of ice supported
 175 by basal water pressure P_w such that $P_w = P_F$ and $h_w = (\rho_I / \rho_w) h_F$ for floating fraction ϕ ,
 176 and my flotation stress $\sigma_F = \sigma_T + \sigma_w = \bar{P}_I \phi^2$ for ice tensile stress σ_T and water buttressing
 177 stress σ_w , all at distance x upstream from an ice-shelf grounding line. At the calving front
 178 of an ice shelf where $\phi = 1$ so $h_F = h_I$ this is identical to the Weertman (1957) and Robin
 179 (1958) solutions. Together σ_T and σ_w resist gravitational forcing linked to \bar{P}_I in an ice
 180 shelf and $\bar{P}_I \phi^2$ linked to floating fraction ϕ in an ice stream at x . My σ_F differs from R_{xx} in
 181 Equation (1) of Van der Veen (2016) because my σ_F always requires basal water deep
 182 enough to uncouple ice from the bed or to supersaturate basal till. In ice streams, water
 183 height h_w above the bed is the height to which basal water would rise in a borehole,
 184 including heights far above sea level (Kamb, 2001).

185 Resistance from my σ_w may be akin to bridging stresses across water-filled cavities
 186 discussed by Van der Veen (2016). The existence of σ_w in the geometric force balance is
 187 not readily apparent from analytic solutions of the Navier-Stokes equations, but Van der
 188 Veen (2016) may have teased it out with his bridging stress, which forces him to add
 189 resistance by including steep shear-stress gradients on each side of his cavities. He
 190 maintains his cavities are small so these gradients average out to zero along an ice stream,
 191 eliminating the need for my σ_w . They cannot average to zero if his cavities are water-filled
 192 and get bigger and closer together downstream, as required to progressively uncouple ice
 193 from the bed. Then cavities themselves have a size and distribution gradient. Figure 1,
 194 which is Figure 4 in Hughes et al. (2016), shows my concept of water-filled cavities in area
 195 $w_I \Delta x$ under an ice stream. We do not know which concept of cavities is correct.

196 **Concluding Remarks**

197 I developed the geometrical force balance over some decades, from Hughes (1992) through
 198 Hughes et al. (2016). My papers are a work in progress, see pages 201-202 of Hughes et al.
 199 (2016) regarding h_w , h_f , σ_w , and σ_f not included in earlier papers. To access my most
 200 recent thinking, see Hughes (2012a) and Hughes et al. (2016). All the earlier studies are
 201 flawed in various ways. The last ones may also have flaws I haven't detected. Some
 202 criticisms by Van der Veen (2016) are directed at my earlier flawed papers.

203 This response gives me an opportunity to correct three mistakes in Hughes (2012a)
 204 that will be apparent to careful readers. The first line in Equation (12.9) should be:

$$205 \quad \partial(\sigma_f h_l) / \partial x = \partial \left[\frac{1}{2} \rho_l g h_l^2 \phi^2 \right] / \partial x = P_l \phi (\phi \alpha_l + h_l \partial \phi / \partial x)$$

206 and in the second line ϕ should be ϕ^2 . In the denominator of Equation (17.18), r should be
 207 replaced by $(a - r)$. The first line of Equation (22.18) should be:

$$208 \quad \Delta h_i^* / \Delta x = \phi^2 \left(\frac{\Delta h_l}{\Delta x} \right)_i + \left(\frac{h_l}{2} \right)_i \frac{\Delta \phi^2}{\Delta x} + \frac{(\tau_o)_i}{\rho_l g h_l^*} + \frac{2(\tau_s)_i}{\rho_l g w_l} = \frac{(\tau_o^*)_i}{\rho_l g h_l^*}$$

209 Equation (22.18) applies to sheet flow when $\phi = \partial \phi / \partial x = 0$ and τ_o^* increases resistance
 210 from basal drag τ_o by including side drag τ_s in flowbands having some side shear. If $\phi > 0$
 211 in tributaries supplying ice streams, and since tributaries are ubiquitous in the sheet-flow
 212 interior of the Antarctic Ice Sheet (Hughes, 2012b), side shear must be taken into account
 213 even for sheet flow because tributaries are flowbands.

214 *Acknowledgements.* I thank Cornelis van der Veen for giving me the opportunity to further
 215 explain my geometric force balance in relation to the standard analytic force balance. I
 216 thank Editor Frank Pattyn for allowing my explanation to appear in *The Cryosphere*. I
 217 especially thank the reviewers, including Van der Veen and Pattyn, who contributed to the
 218 Interactive Discussion. As always, reviewers are worth their weight in gold.

219 **References**

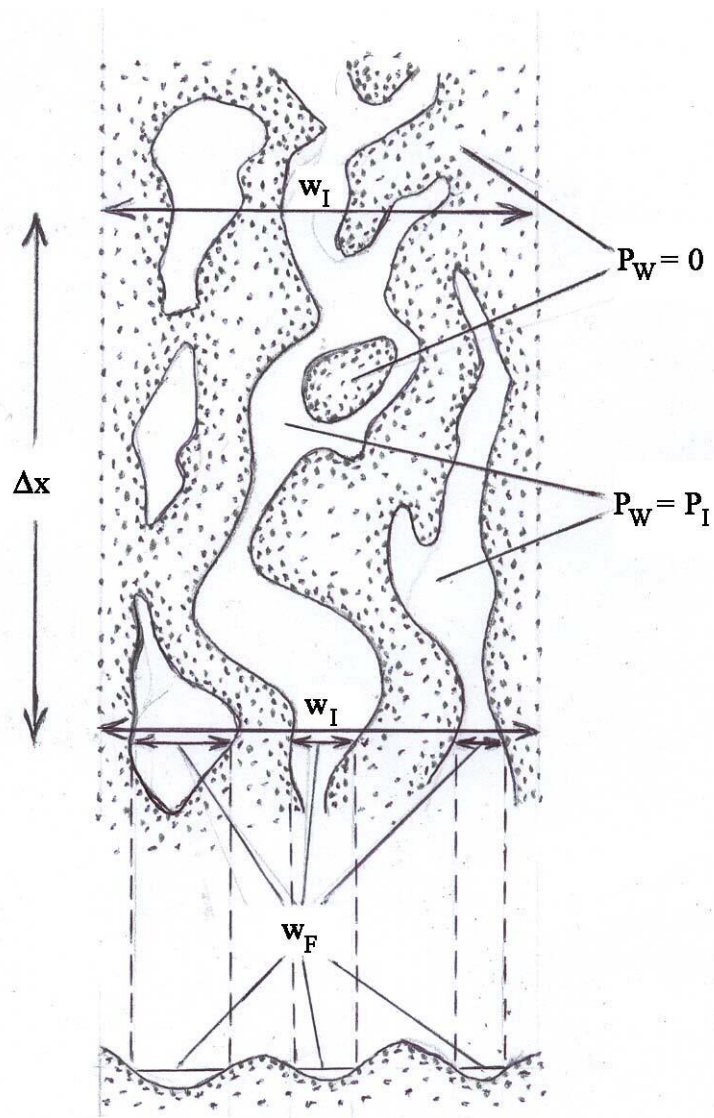
- 220 Denton, G.H., and Hughes, T.J., Eds.: The Last Great Ice Sheets. New York: Wiley
 221 Interscience, 484 pages, 1981.
- 222 Fastook, J.L., and Hughes, T.J.: New perspectives on paleoglaciology. *Quat. Sci. Rev.*, 80, 169-
 223 194, 2013.
- 224 Hughes, T.J.: Ice Sheets. Oxford, U.K., Oxford Univ. Press, 343 pages, 1998.
- 225 Hughes, T.: On the pulling power of ice streams. *J. Glaciol.*, 38, 125-151, 1992.
- 226 Hughes, T.: Holistic Ice Sheet Modeling: A First-Order Approach. New York: Nova
 227 Publishers, 261 pp., 2012a.

- 228 Hughes, T.: Are ice-stream tributaries the surface expression of thermal convection rolls in
229 the Antarctic ice sheet? *J. Glaciol.* 58(210), 811-814, 2012b.
- 230 Hughes, T., Sargent, A., Fastook, J., Purdon, K., Li, J., Yan, J.-B., and Gogineni, S.: Sheet, stream,
231 and shelf flow as progressive ice-bed uncoupling: Byrd Glacier, Antarctica and
232 Jakobshavn Isbrae, Greenland. *The Cryosphere*, 10, 193-225, doi:10.5194/tc-10- 193-
233 2016, 2016.
- 234 Kamb, B.: Basal zone of the West Antarctic ice streams and its role in lubrication of their
235 rapid motion, in: *The West Antarctic Ice Sheet: Behavior and Environment*, edited by
236 Alley, R.B., and Bindshadler, R.A., Antarctic Research Series, American Geophysical
237 Union, Washington, D.C., 157-200, 2001.
- 238 Raymond, C.F.: Deformation in the vicinity of ice divides. *J. Glaciol.*, 29(103), 357-373, 1983.
- 239 Robin, G. deQ.: Glaciology III: Seismic shooting and related investigations. *Scientific Results*
240 *of the Norwegian, British, Swedish Antarctic Expedition, 1949-1952*, 5, 111-125, 1958.
- 241 Siegert, M.J.: Comments on “calculating basal thermal zones beneath the Antarctic Ice
242 Sheet” by Wilch and Hughes (letter). *J. Glaciol.*, 47(156), 159-160, 2001.
- 243 Van der Veen, C.J.: Basal buoyancy and fast-moving glaciers: in defense of analytic force
244 balance. *The Cryosphere*, 10, 1331-1337, 2016.
- 245 Weertman, J.: Deformation of floating ice shelves. *J. Glaciol.*, 3(21), 38-42, 1957.
- 246 Wilch, E., and Hughes, T., Mapping basal thermal zones beneath the Antarctic ice sheet. *J.*
247 *Glaciol.*, 46(153), 297-310, 2000.

248 **Table 1:** Resisting Stresses Linked to Floating Fraction $\phi = P_F/P_I$ of Ice and Gravitational
 249 Forces Numbered in Figure 2 for the Geometrical Force Balance.

Basal water pressure at x , from gravity force 3: $P_W = \rho_W g h_W$
Ice overburden pressure at x , from gravity force (1+2+3+4): $P_I = \rho_I g h_I$
Upslope tensile stress at x , from gravity force 4: $\sigma_T = \bar{P}_I (1 - \rho_I / \rho_W) \phi^2$
Downslope compressive stress at x due to $\bar{\tau}_O$ and $\bar{\tau}_S$ along x and σ_W at $x = 0$: $\sigma_C = \bar{P}_I - \sigma_T = \bar{P}_I - \bar{P}_I (1 - \rho_I / \rho_W) \phi^2$
Downslope water-pressure stress at x , from gravity force 3: $\sigma_W = \bar{P}_I (\rho_I / \rho_W) \phi^2$
Upslope flotation stress at x from gravity force (3+4): $\sigma_F = \sigma_T + \sigma_W = \bar{P}_I \phi^2$
Longitudinal force balance at x from gravity force [(5+6+7+8)-(1+2+3+4)]: $P_I \alpha = \partial(\sigma_F h_I) / \partial x + \tau_O + 2\tau_S (h_I / w_I)$
Flotation force gradient at x from gravity force [(7+8)-(3+4)]: $\partial(\sigma_F h_I) / \partial x = P_I \phi (\phi \alpha_I + h_I \partial \phi / \partial x)$
Basal shear stress at x from gravity force (5-1): $\tau_O = P_I (1 - \phi)^2 \alpha - P_I h_I (1 - \phi) \partial \phi / \partial x$
Side shear stress at x from gravity force (6-2): $\tau_S = P_I (w_I / h_I) \phi (1 - \phi) \alpha + \bar{P}_I w_I (1 - 2\phi) \partial \phi / \partial x$
Average downslope basal shear stress to x from gravity force 1: $\bar{\tau}_O = \bar{P}_I w_I h_I (1 - \phi)^2 / (w_I x + A_R)$
Average downslope side shear stress to x from gravity force 2: $\bar{\tau}_S = P_I w_I h_I \phi (1 - \phi) / (2\bar{h}_I x + 2L_S \bar{h}_S + C_R \bar{h}_R)$

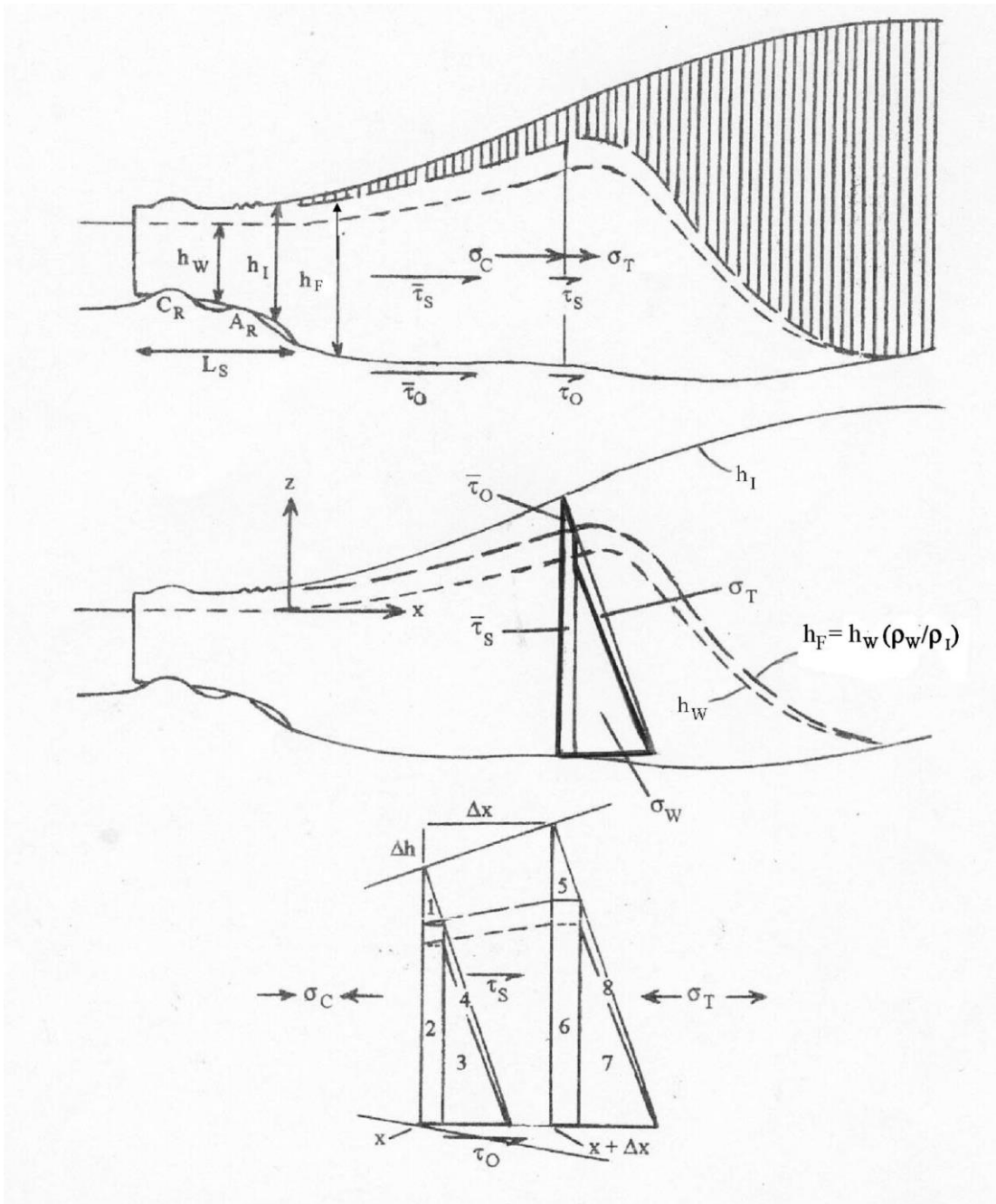
250



251

252 Figure 1: Figure 4 from Hughes et al. (2016). Under an ice stream, basal ice is grounded in
 253 the shaded areas and floating in the unshaded areas (top) as seen in a transverse cross-
 254 section (bottom) for incremental basal area $w_I \Delta x$.

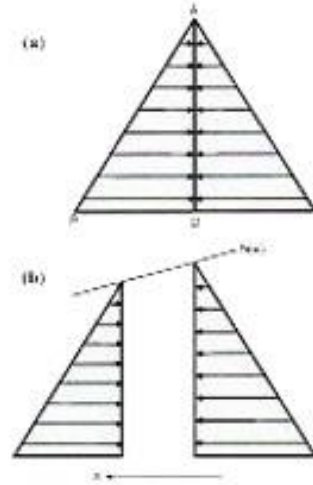
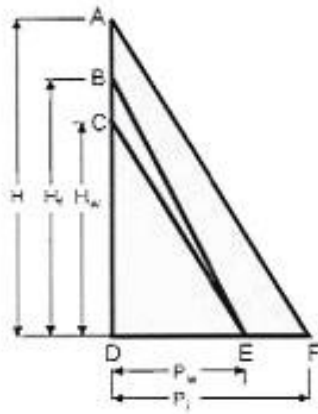
255



256

257 Figure 2: Figure 5 from Hughes et al. (2016). Top: Stresses at x and downstream from x that
 258 resist gravitational forcing. The bed supports ice in the shaded area. Middle: The
 259 gravitational force inside the thick border is linked to σ_C which represents all
 260 downstream resistance to ice flow at point x . Bottom: Gravitational forces (geometrical
 261 areas 1 through 8) and resisting stresses along incremental downstream length Δx at
 262 point x .

263



264

265

Figure 3: Figure 3 (left) and Figure 4 (right) from Van der Veen (2016).